White X-ray Topography Combined with a Topo-tomographic Technique for Determining Three-dimensional Dislocation Structures in Silicon

A three-dimensional characterization of lattice imperfections in single crystals has often been required in X-ray topography studies. The topo-tomography technique, which was devised by Ludwig *et al.* [1] to analyze the configuration of individual dislocations, is extremely sophisticated. However, due to a lack of information regarding the image contrast, this technique is insufficient for determining the nature of individual dislocations, such as Burgers vectors and glide planes. Recently, we demonstrated that a combination of white X-ray topography and the topo-tomographic technique is a useful tool for the determination of the three-dimensional structure of the individual dislocations in silicon, i.e., the direction of the dislocation line, its Burgers vector and the glide plane [2]. The advantage of this method lies in its ability to acquire information regarding the configuration of the dislocations from the variation in their features observed in a specific Laue spot by the tomographic technique, in addition to information regarding the image contrast of the dislocations observed in several Laue spots by conventional white X-ray topography.

The production of large-scale integrated circuits in the future will require large-diameter Czochralski silicon crystals. Research and development of the crystal growth technology without Dash necking is required because the weight of a crystal with a diameter of 400 mm exceeds 400 kg. It is well known that dislocations are generated when the seed comes into contact with the melt, whereas the mechanism of the elimination of dislocations during the Dash necking process is still unclear [3].

In order to elucidate this mechanism, the determination of the three-dimensional structure of dislocations in the neck of a silicon crystal of 2-inch diameter, which was grown in the laboratory, was carried out at beamline **BL28B2** [4]. Figure 1 shows the experimental setup. The sample crystal was fixed, by positioning its growth axis [001] nearly parallel to the ω-axis, on the sample holder of the subsidiary goniometer that was mounted on the swivel stage of the main diffractometer.

On the basis of an *in situ* observation of the transmission Laue patterns, the orientation of the sample was adjusted such that the (100) plane was perpendicular to the incident X-ray beam, and the [010] orientation was horizontal. This angular position

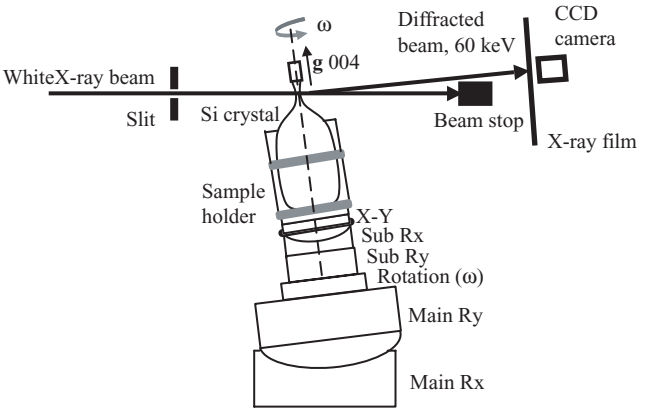

Fig. 1. Schematic illustration of the experimental arrangement. The subsidiary goniometer comprises a sample holder, and *x-y*, *Rx*, *Ry* and ω-rotation stages. Only the *Rx* and *Ry* swivel stages of the main diffractometer are drawn.

was designated as ω = 0º. Therefore, when ω = 45, 90 and 135º, the plane perpendicular to the incident X-ray beam corresponded to (110), (010) and $(\bar{1}10)$, respectively. The sample was inclined by 4.36º (Bragg angle), using the *Rx* stage of the main diffractometer, such that the 004 Laue spot could be formed by 60 keV X-rays. Finally, the growth axis [001] of the sample crystal was precisely adjusted so as to be parallel to the ω-axis. After the adjustment was completed, the 004 Laue spot was recorded, by rotating the ω-axis at intervals of 3º, onto the hard disk of a personal computer connected to a cooled CCD camera. In addition, several sets of Laue patterns were recorded on the X-ray films at ω-intervals of 45º.

The first step in the dislocation-structure analysis was to maintain a check on the variation in the features of individual dislocations owing to the ω-rotation, by reproducing their CCD images, in order to clarify the configuration of each dislocation and identify its images in the 004 spot obtained at ω = 0, 45, 90, and 135º. The second step was to determine their Burgers vectors from the variation in the contrast of their images in several Laue spots that were recorded on the X-ray film at each ω-angle. The final step was to fix glide planes on the basis of both the configuration of the dislocations clarified in the first step and the Burgers vectors determined in the second step.

The ω-dependence of the enlarged images in the

004 spot obtained from the neck region of the sample crystal is shown in Fig. 2(a). Dislocation half-loops as well as tangled dislocations are observed in these images. Figure 2(b) shows the enlarged images of the $\bar{1}\bar{1}1$, 111, $\bar{1}11$ and $1\bar{1}1$ spots. Five representative dislocations, designated as A, B, C, D, and E, were analyzed, and the results are summarized in Table 1 and Fig. 3. The present observation revealed that dislocation half-loops, which were generated from tangled dislocations formed near the interface of the seed and the grown crystal, were expanded on the {111} glide planes. The elimination of dislocations due to Dash necking was caused by the termination of the expansion of the dislocation half-loops inside the crystal and by pinning the dislocations on the crystal surface.

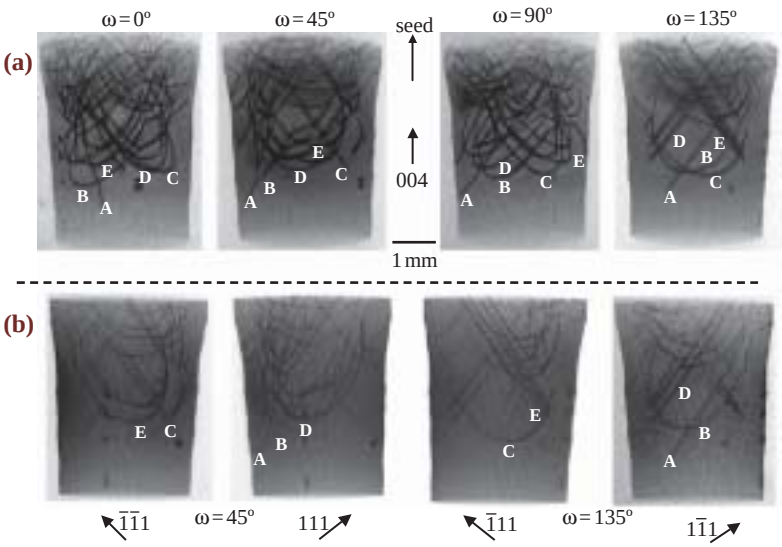

Fig. 2. **(a)** A series of enlarged images in the 004 spot obtained at ω = 0, 45, 90 and 135°. **(b)** Enlarged images of the $\bar{1}\bar{1}1$ and 111 spots obtained at ω = 45° and those of the $\bar{1}11$ and $1\bar{1}1$ spots obtained at ω = 135°.

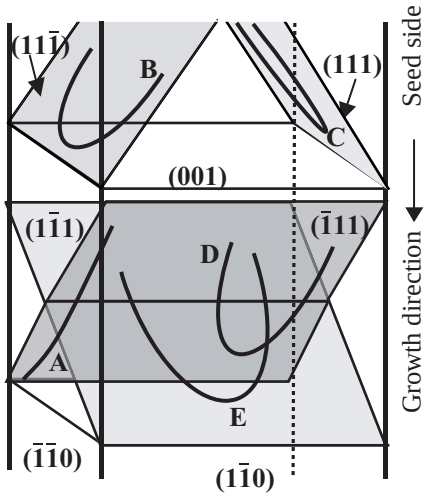

Fig. 3. Schematic illustration of dislocations designated as A, B, C, D and E. Dislocations A and D do not lie on the same ($\bar{1}$11) plane. Such a representation is adopted so as to avoid unnecessary complications.

Table 1. Identification of observed dislocations.

Dislocation image	shape	Laue spot invisible or weak		Burgers vector	Glide plane
A	straight	$\bar{1}\,\bar{1}\,1$	$\bar{1}\,1\,1$	**a**/2[1 0 1]	($\bar{1}$ 1 1)
B	curved	$\bar{1}\,\bar{1}\,1$	$\bar{1}\,1\,1$	**a**/2[1 0 1]	(1 1 $\bar{1}$)
C	curved	1 1 1	1 $\bar{1}$ 1	**a**/2[1 0 $\bar{1}$]	(1 1 1)
D	curved	$\bar{1}\,\bar{1}\,1$	$\bar{1}\,1\,1$	**a**/2[1 0 1]	($\bar{1}$ 1 1)
E	curved	1 1 1	1 $\bar{1}$ 1	**a**/2[1 0 $\bar{1}$]	(1 $\bar{1}$ 1)

Seiji Kawado[a,*], Satoshi Iida[b] and Yoshinori Chikaura[c]

(a) X-Ray Research Laboratory, Rigaku Corporation
(b) Faculty of Science, Toyama University
(c) Graduate School of Engineering, Kyushu Institute of Technology

*E-mail: kawado@rigaku.co.jp

References

[1] W. Ludwig *et al.*: J. Appl. Cryst. **34** (2001) 602.
[2] S. Kawado *et al.*: J. Synchrotron Rad. **11** (2004) 304.
[3] Y. Wang and K. Kakimoto: J. Crystal Growth **247** (2003) 1.
[4] *S. Kawado, T. Taishi, S. Iida, Y. Suzuki, Y. Chikaura and K. Kajiwara: J. Phys. D: Appl. Phys.* ***38*** *(2005) A17.*